

# Coupling of Higgs and Leggett modes in nonequilibrium superconductors

H. Krull,<sup>1,\*</sup> N. Bittner,<sup>2,†</sup> G. S. Uhrig,<sup>1,‡</sup> D. Manske,<sup>2,§</sup> and A. P. Schnyder<sup>2,¶</sup>

<sup>1</sup>*Lehrstuhl für Theoretische Physik I, Technische Universität Dortmund,  
Otto-Hahn Straße 4, 44221 Dortmund, Germany*

<sup>2</sup>*Max-Planck-Institut für Festkörperforschung, Heisenbergstraße 1, D-70569 Stuttgart, Germany*  
(Dated: December 29, 2015)

Collective excitation modes are a characteristic feature of symmetry-broken phases of matter. For example, superconductors exhibit an amplitude Higgs mode and a phase mode, which are the radial and angular excitations in the Mexican-hat potential of the free energy. In two-band superconductors there exists in addition a Leggett phase mode, which corresponds to collective fluctuations of the interband phase difference. In equilibrium systems amplitude and phase modes are decoupled, since they are mutually orthogonal excitations. The direct detection of Higgs and Leggett modes by linear-response measurements is challenging, because they are often overdamped and do not couple directly to the electromagnetic field. In this work, using numerical exact simulations we show for the case of two-gap superconductors, that optical pump-probe experiments excite both Higgs and Leggett modes out of equilibrium. We find that this non-adiabatic excitation process introduces a strong interaction between the collective modes. Moreover, we predict that the coupled Higgs and Leggett modes are clearly visible in the pump-probe absorption spectra as oscillations at their respective frequencies.

Ultrafast pump-probe measurements have become a key tool to probe the temporal dynamics and relaxation of quantum materials. This technique has proven to be particularly valuable for the study of order parameter dynamics in symmetry-broken states, such as superconductors [1–9], charge-density-waves [10, 11], and antiferromagnets [12]. In these experiments the pump laser pulse excites a high density of quasiparticles above the gap of the order parameter, thereby modifying the Mexican-hat potential of the free energy  $\mathcal{F}$ . As a result, the amplitude of the order parameter decreases, reducing the minimum of the free energy. If the pump-pulse induced changes in  $\mathcal{F}$  occur on a faster time scale than the intrinsic response time of the symmetry-broken state, the collective modes start to oscillate at their characteristic frequencies about the new free-energy minimum [see Fig. 1(a)]. This

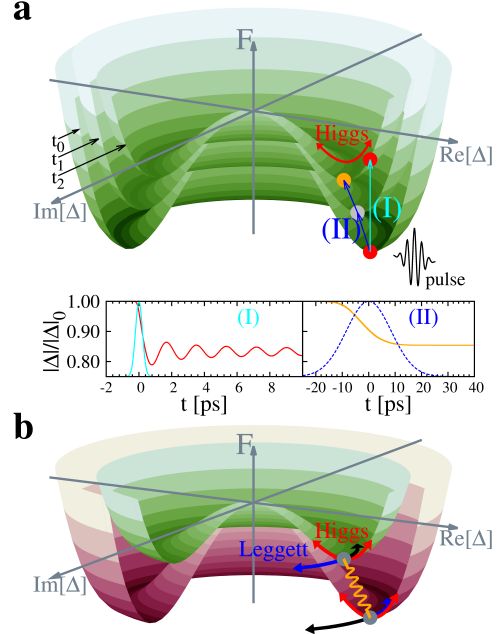


FIG. 1. **Illustration of Leggett and Higgs modes.** (a) Illustration of the excitation process for a one band superconductor. The pump laser pulse modifies the free energy  $\mathcal{F}$  on different time scales depending on the pulse duration  $\tau$ . For  $\tau \gg \hbar/(2|\Delta|)$  the superconductor can follow the change in  $\mathcal{F}$  adiabatically, resulting in a monotonic lowering of the order parameter  $|\Delta|$  [inset (II)]. For short pulses with  $\tau \lesssim \hbar/(2|\Delta|)$ , on the other hand, the superconductor is excited in a non-adiabatic fashion, which results in oscillations of  $|\Delta|$  about the new minimum of  $\mathcal{F}$  [inset (I)]. The blue and cyan lines in the two insets represent the Gaussian profiles of the pump pulses. (b) Effective free-energy landscape  $\mathcal{F}$  for a two-gap superconductor, with green and red representing the Mexican-hat potentials of the smaller and larger gaps, respectively. The amplitude Higgs modes and the phase modes are indicated by red and blue/black arrows, respectively. The Leggett mode corresponds to out-of-phase fluctuations of the phase difference between the two gaps.

non-adiabatic excitation mechanism has recently been demonstrated for the amplitude Higgs mode of the one-gap superconductor NbN. It has been shown, both theoretically [13–26] and experimentally [1–3], that a short intense laser pulse of length  $\tau$  much shorter than the dynamical time scale of the superconductor  $\tau_\Delta \simeq \hbar/(2|\Delta|)$  induces oscillations in the order parameter amplitude at the frequency  $\omega_H = 2\Delta_\infty/\hbar$ , with  $\Delta_\infty$  the asymptotic

\* holger.krull@tu-dortmund.de

† n.bittner@fkf.mpg.de

‡ goetz.uhrig@tu-dortmund.de

§ d.manske@fkf.mpg.de

¶ a.schnyder@fkf.mpg.de

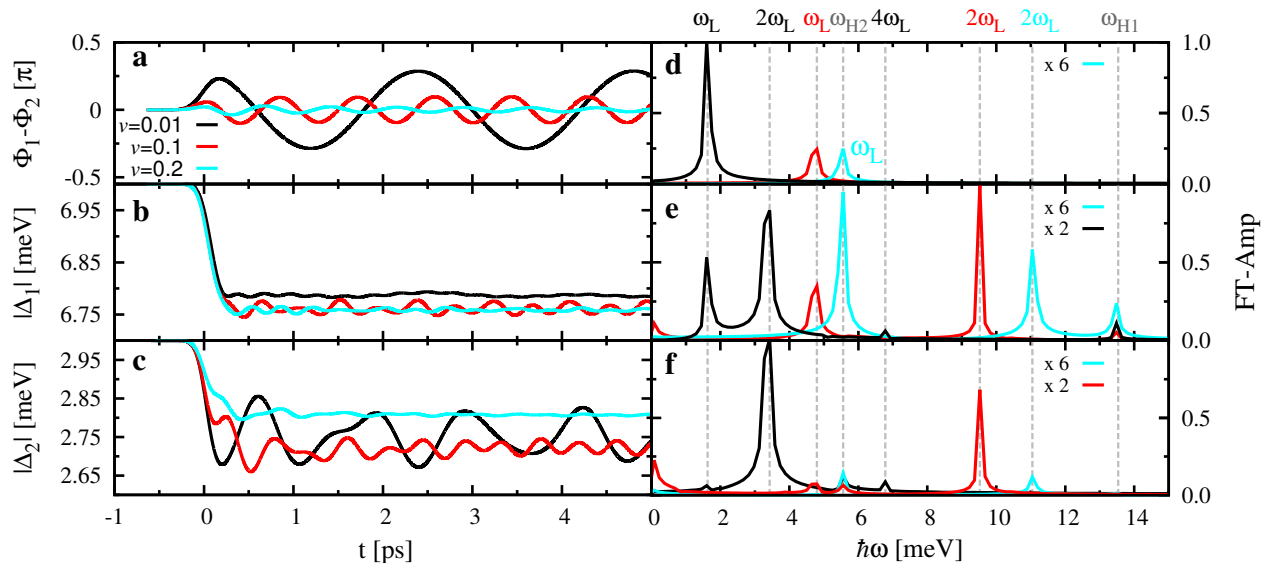


FIG. 2. **Leggett phase mode and amplitude Higgs mode oscillations.** Numerical simulation of the gap dynamics of a two-gap superconductor after a non-adiabatic excitation by a short intense laser pulse of width  $\tau = 0.4$  ps, pump energy  $\hbar\omega_0 = 8$  meV, and light-field amplitude  $|\mathbf{A}_0| = 10 \cdot 10^{-8}$  Js/(Cm). (a) Phase difference  $\Phi_1 - \Phi_2$  between the two gaps as a function of time  $t$  for various interband coupling strengths  $v$ . (d) Fourier spectrum of the oscillations in panel (a). The frequency of the nonequilibrium Leggett mode oscillation is indicated by  $\omega_L$ . (b), (c) Gap amplitudes  $|\Delta_1|$  and  $|\Delta_2|$  as a function of time  $t$  for different interband couplings  $v$ . (e), (f) Fourier spectra of the amplitude mode oscillations in panels (b), (c), which display the following frequencies:  $\omega_{H1}$  and  $\omega_{H2}$  the frequencies of the nonequilibrium Higgs modes of gap  $\Delta_1$  and  $\Delta_2$ , respectively;  $\omega_L$  the frequency of the nonequilibrium Leggett mode; and higher harmonics of the nonequilibrium Leggett mode denoted by  $2\omega_L$  and  $4\omega_L$ .

gap value.

While nonequilibrium collective modes in conventional single-gap superconductors are well understood, the investigation of collective excitations in unconventional nonequilibrium superconductors with multiple gaps, such as MgB<sub>2</sub> or iron pnictides, is still in its infancy [27–29]. These multicomponent superconductors have a particularly rich spectrum of collective excitations [30–32]. In this paper, we simulate the pump-probe process in a two-gap superconductor using a semi-numerical approach based on the density-matrix formalism. This method is exact for mean-field Hamiltonians [14, 20], captures the coupling between the superconductor and the electromagnetic field of the pump laser at a microscopic level, and allows for the calculation of the pump-probe conductivity, as measured in recent experiments [1, 2]. Two-gap superconductors exhibit besides the amplitude Higgs [33] and the phase modes [34, 35], also a Leggett mode [30], which results from fluctuations of the relative phase of the two coupled gaps, i.e., equal but opposite phase shifts of the two order parameters, see Fig. 1(b). In equilibrium superconductors, the Higgs and Leggett modes are decoupled, since they correspond to mutually orthogonal fluctuations. In contrast to the phase mode, both Higgs and Leggett modes are charge neutral and therefore do not couple directly to the electromagnetic field [36]. This has made it difficult to directly detect these excitations with standard linear-response type measurements [37–40].

Here, we show that in a pump-probe experiment both Leggett and Higgs modes can be excited out of equilibrium, and directly observed as oscillations in the absorption spectra at their respective frequencies. We find that the non-adiabatic excitation process of the pump pulse induces an intricate coupling between the two charge-neutral modes, which pushes the frequency of the Leggett mode below the continuum of two-particle excitations. Moreover, the frequencies of the Leggett and Higgs modes and the coupling between them can be controlled by the fluence of the pump pulse. Hence, by adjusting the laser intensity the two modes can be brought into resonance, which greatly enhances their oscillatory signal in the pump-probe absorption spectra.

## Results

In this work we use numerical exact simulations in order to study the nonequilibrium response of two-gap superconductors perturbed by a short and intense pump pulse. The Hamiltonian describing the superconductor coupled to the pump laser field is given by  $H = H_{\text{BCS}} + H_{\text{laser}}$ , with the two-band BCS mean-field Hamiltonian

$$H_{\text{BCS}} = H_0 + \sum_{\mathbf{k} \in \mathcal{W}} \sum_{l=1}^2 \left( \Delta_l c_{\mathbf{k}l\uparrow}^\dagger c_{-\mathbf{k}l\downarrow}^\dagger + \Delta_l^* c_{-\mathbf{k}l\downarrow} c_{\mathbf{k}l\uparrow} \right), \quad (1)$$

where  $H_0 = \sum_{\mathbf{k}l\sigma} \varepsilon_{\mathbf{k}l} c_{\mathbf{k}l\sigma}^\dagger c_{\mathbf{k}l\sigma}$  denotes the normal state Hamiltonian and  $c_{\mathbf{k}l\sigma}^\dagger$  creates electrons with momentum  $\mathbf{k}$ , band index  $l$ , and spin  $\sigma$ . The first sum in Eq. (1)

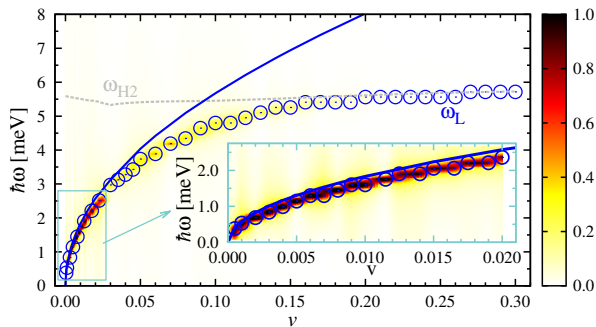


FIG. 3. **Leggett phase mode oscillations vs. relative interband coupling.** Fourier spectrum of the phase mode  $\Phi_1 - \Phi_2$  as a function of relative interband coupling  $v$  for a two-band superconductor perturbed by the same laser pulse as in Fig. 2. The amplitude of the phase fluctuations is indicated by the color scale with dark red and light yellow representing the highest and lowest amplitudes, respectively. The blue open circles mark the frequency of the nonequilibrium Leggett mode  $\omega_L$ . The blue solid line represents the frequency of the equilibrium Leggett mode described by equation (2). The dashed gray line indicates the frequency of the Higgs mode  $\omega_{H2}$ , which coincides with the boundary to the continuum of Bogoliubov quasiparticle excitations, given by twice the asymptotic gap value of the second band  $2\Delta_2^\infty$ . The inset shows a zoom-in of the blue frame in the main panel.

is taken over the set  $\mathcal{W}$  of momentum vectors with  $|\varepsilon_{\mathbf{k}l}| \leq \hbar\omega_c = 50$  meV,  $\omega_c$  being the cut-off frequency. The gaps  $\Delta_1$  and  $\Delta_2$  in the two bands are determined at each temporal integration step from the BCS gap equations with the attractive intraband pairing interactions  $V_1$  and  $V_2$  and the interband coupling  $V_{12} = vV_1$ . We fix  $V_1$  and  $V_2$  such that the gaps in the initial state take on the values  $\Delta_1(t_i) = 7$  meV and  $\Delta_2(t_i) = 3$  meV, and study the dynamics of the two-gap superconductor as a function of the relative interband coupling  $v$ .  $H_{\text{laser}}$  represents the interaction of the pump laser with the superconductor and contains terms linear and quadratic in the vector potential of the laser field, which is of Gaussian shape with central frequency  $\hbar\omega_0 = 8$  meV, pulse width  $\tau = 0.4$  ps, and light-field amplitude  $|\mathbf{A}_0|$ . We determine the dynamics of Hamiltonian (1) by means of the density matrix approach and solve the resulting equations of motion using Runge-Kutta integration (see Methods).

**Pump response.** Pumping the two-band superconductor with a short laser pulse of length  $\tau \ll \tau_\Delta$  excites a nonthermal distribution of Bogoliubov quasiparticles above the gaps  $\Delta_i$ , which in turn leads to a rapid, non-adiabatic change in the free-energy landscape  $\mathcal{F}$ . As a result, the collective modes of the superconductor start to oscillate about the new minima of  $\mathcal{F}$ . This is clearly visible in Fig. 2, which shows the temporal evolution of the gap amplitudes  $|\Delta_i|$  and of the phase difference  $\Phi_1 - \Phi_2$  between the two gaps. From the Fourier spectra in Figs. 2(d)-(f) we can see that three different modes (and their higher harmonics) are excited at the frequen-

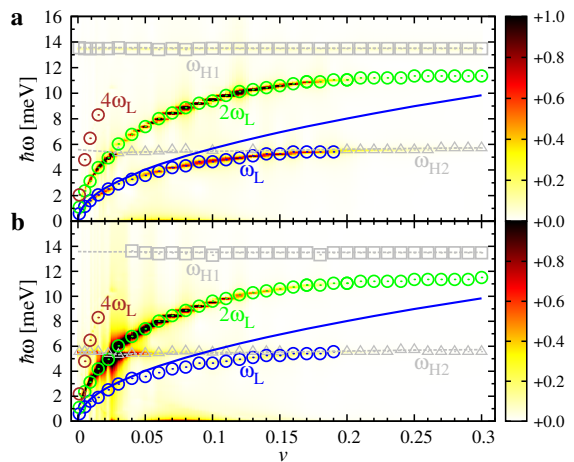


FIG. 4. **Amplitude mode oscillations vs. relative interband coupling.** Fourier spectrum of the amplitude mode oscillations as a function of relative interband coupling  $v$  for (a) the superconducting gap  $\Delta_1$  in the first band and (b) the superconducting gap  $\Delta_2$  in the second band. The parameters of the laser pump pulse are the same as in Fig. 2. The amplitude of the oscillations is indicated by the color scale with dark red and light yellow representing the highest and lowest amplitudes, respectively. The open circles represent the frequencies of the nonequilibrium Leggett mode  $\omega_L$  and its higher harmonics denoted by  $2\omega_L$  and  $4\omega_L$ . The frequencies of the nonequilibrium Higgs mode of the first and second band,  $\omega_{H1}$  and  $\omega_{H2}$ , are indicated by the grey open squares and triangles, respectively. The blue solid line is the frequency of the equilibrium Leggett mode given by equation (2).

cies  $\omega_{H1}$ ,  $\omega_{H2}$ , and  $\omega_L$ . The two modes at  $\omega_{H1}$  and  $\omega_{H2}$  only exist in the dynamics of  $\Delta_1(t)$  and  $\Delta_2(t)$ , respectively, and their peaks are located at the energy of the superconducting gaps  $\omega_{Hi} = 2|\Delta_i^\infty|/\hbar$ , where  $\Delta_i^\infty$  denotes the asymptotic gap value [13–19]. This holds for all parameter regimes, even as the laser fluence is increased far beyond the linear absorption region (see Fig. 5). We therefore assign the peaks at  $\omega_{H1}$  and  $\omega_{H2}$  to the Higgs amplitude modes of the two gaps. The higher Higgs mode  $\omega_{H1}$  is strongly damped, because it lies within the continuum of Bogoliubov quasiparticle excitations, which is lower bounded by  $2\Delta_2^\infty$ . For the lower mode  $\omega_{H2}$ , on the other hand, the decay channel to quasiparticles is small, since  $\omega_{H2}$  is at the continuum threshold. This is similar to the nonequilibrium Higgs mode of the single-gap superconductor NbN, whose oscillations have recently been observed over a time period of about 10 ps by pump-probe measurements [1, 2].

Interestingly, two-band superconductors exhibit a third collective mode besides the two Higgs modes at a frequency  $\omega_L$  below the quasiparticle continuum. This mode is most clearly visible in the dynamics of the phase difference  $\Phi_1 - \Phi_2$  [Fig. 2(a)] and displays a striking dependence on interband coupling strength  $v$ . With decreasing  $v$  its frequency rapidly decreases, while its in-

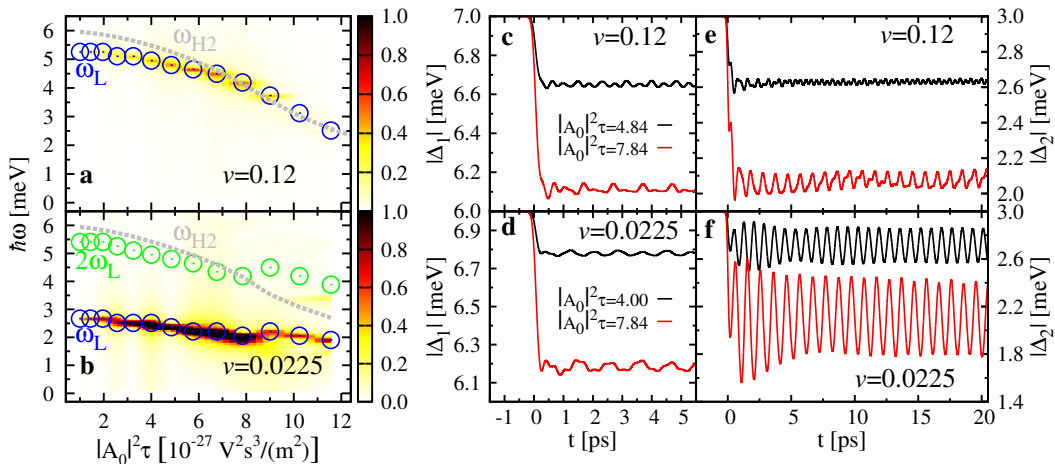


FIG. 5. **Fluence dependence of gap dynamics.** (a), (b) Fourier spectrum of the phase mode  $\Phi_1 - \Phi_2$  as a function of laser fluence (integrated pulse intensity)  $|\mathbf{A}_0|^2\tau$  for two different interband couplings  $v$  with pulse energy  $\hbar\omega_0 = 8$  meV and pulse width  $\tau = 0.4$  ps. The amplitude of the phase fluctuations is represented by the color scale with dark red and light yellow indicated high and low amplitudes, respectively. The open circles mark the frequencies of the nonequilibrium Leggett mode  $\omega_L$  and its higher harmonic  $2\omega_L$ . The grey dotted lines display the Higgs-mode  $\omega_{H2}$ , which coincides with the boundary to the continuum of Bogoliubov quasiparticle excitations. (c) – (f) Gap amplitudes  $|\Delta_1|$  and  $|\Delta_2|$  as a function of time  $t$  for two different interband couplings  $v$  and integrated pulse intensities  $|\mathbf{A}_0|^2\tau$ .

tensity grows. In the limit of vanishing  $v$ , however, the third mode  $\omega_L$  is completely absent. We thus identify  $\omega_L$  as the Leggett phase mode, i.e., as equal but opposite oscillatory phase shifts of the two coupled gaps. Remarkably, the Leggett phase mode is also observable in the time dependence of the gap amplitudes  $\Delta_1(t)$  and  $\Delta_2(t)$  [Figs. 2(b) and 2(c)], which indicates that Higgs and Leggett modes are coupled in nonequilibrium superconductors.

To obtain a more detailed picture, we plot in Figs. 3 and 4 the energies of the amplitude and phase mode oscillations against the relative interband coupling  $v$ . This reveals that for small  $v$  the nonequilibrium Leggett mode  $\omega_L$  shows a square root increase, which is in good agreement with the equilibrium Leggett frequency [30, 41]

$$\omega_L^0 = 2\sqrt{\Delta_1^\infty \Delta_2^\infty \frac{v}{V_1 V_2 - v^2} \left( \frac{1}{\rho_1} + \frac{1}{\rho_2} \right)}, \quad (2)$$

where  $\rho_1$  and  $\rho_2$  denote the density of states on the two bands. Indeed, as displayed by the inset of Fig. 3, Eq. (2) represents an excellent parameter-free fit to the numerical data at low  $v$ . For larger  $v$ , on the other hand, the nonequilibrium Leggett mode deviates from the square root behavior of Eq. (2). That is, as  $\omega_L$  approaches the Bogoliubov quasiparticle continuum, it is repelled by the lower Higgs mode  $\omega_{H2}$ , evidencing a strong coupling between them. As a result, the nonequilibrium Leggett mode is pushed below the continuum and remains nearly undamped for a wide range of  $v$ , which is considerably broader than in equilibrium. Moreover, due to the dynamical coupling among the collective modes,  $\omega_L$  and its higher harmonics are observable not only in the phase difference  $\Phi_1 - \Phi_2$ , but also in the dynamics of the gap

amplitudes  $\Delta_i(t)$  (blue and green circles in Fig. 4).

A key advantage of measuring collective modes by pump-probe experiments, is that the frequencies of the Higgs modes can be adjusted by the pump fluence. This is demonstrated in Fig. 5, which plots the dynamics of  $\Delta_i(t)$  and  $\Phi_1 - \Phi_2$  as a function of integrated pump pulse intensity  $|\mathbf{A}_0|^2\tau$ . With increasing pump fluence, more Cooper pairs are broken up and superconductivity is more and more suppressed, as reflected in the reduction of the gap amplitudes. At the same time, the frequency of the Higgs oscillations decreases, since it is controlled by the superconducting gaps after pumping. Hence, it is possible to tune the lower Higgs mode  $\omega_{H2}$  to resonance with  $\omega_L$ , which strongly enhances the magnitude of the collective-mode oscillations [Figs. 5(a), 5(c), and 5(e)]. A similar enhancement is obtained when  $\omega_{H2}$  is brought into resonance with twice the frequency of the Leggett mode [Figs. 5(b), 5(d), and 5(f)].

**Pump-probe signal.** Finally, let us discuss how the Higgs and Leggett modes can be observed in pump-probe spectroscopy. In view of the recent THz pump-THz probe experiments of Refs. [1–3], we focus on the dynamics of the optical pump-probe conductivity  $\sigma(\delta t, \omega) = j(\delta t, \omega)/[i\omega A(\delta t, \omega)]$ , where  $\delta t$  is the delay time between pump and probe pulses,  $j(\delta t, \omega)$  denotes the current density, and  $A(\delta t, \omega)$  represents the vector potential of the probe pulse. Since the probe pulse has a weak intensity, we neglect terms of second order and higher in the probe field  $A(\delta t, \omega)$ . Similar to recent experiments [1–6], we take the probe pulse to be very short with width  $\tau_{pr} = 0.15$  ps and center frequency  $\hbar\omega_{pr} = 5.5$  meV (see Methods). With this choice, the probe pulse has a broad spectral bandwidth such that the dynamics of the super-

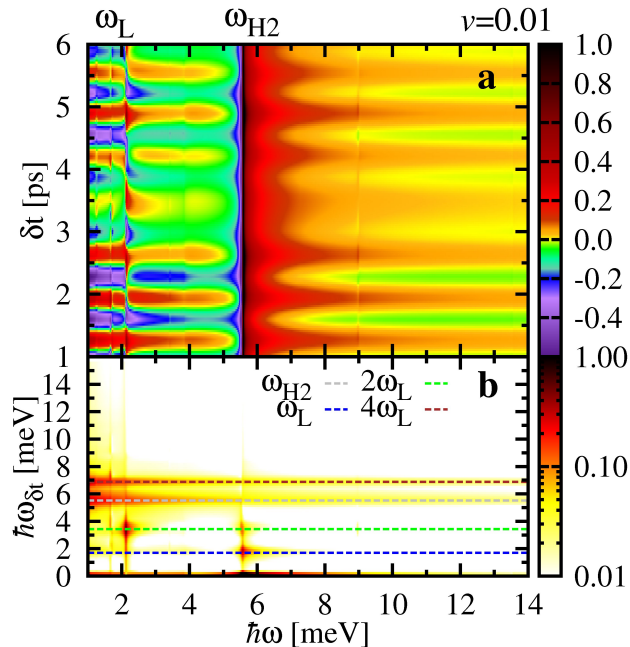


FIG. 6. **Pump-probe spectrum.** (a) Temporal evolution of the real part of the pump-probe response  $\text{Re}[\sigma(\delta t, \omega)]$  for a two-band superconductor excited by the same pump pulse as in Fig. 2. The intensity of the pump-probe signal is represented by the color scale with dark red and dark violet indicating high and low intensities, respectively. Both the energy of the non-equilibrium Leggett mode  $\omega_L$  and the Higgs-mode  $\omega_{H2}$  are visible in the pump-probe signal as sharp peaks. (b) Fourier spectrum of the pump-probe signal. The pump-probe spectrum oscillates as a function of pump-probe delay time  $\delta t$  with the frequencies of the nonequilibrium Higgs mode  $\omega_{H2}$  (dashed gray), the frequency of the nonequilibrium Leggett mode  $\omega_L$  (dashed blue), and the frequencies of higher harmonics of the Leggett mode  $2\omega_L$  (dashed green) and  $4\omega_L$  (dashed red).

conductor is probed over a very wide frequency range.

In Fig. 6(a) we plot the real part of the pump-probe response  $\text{Re}[\sigma(\delta t, \omega)]$  versus delay time  $\delta t$  and frequency  $\omega$ . Clear oscillations are seen as a function of delay time  $\delta t$ . These are most prominent at the frequencies of the lower Higgs and the Leggett modes,  $\omega_{H2}$  and  $\omega_L$ , where  $\sigma(\delta t, \omega)$  displays sharp edges as a function of  $\omega$ . Fourier transforming with respect to  $\delta t$  shows that the dominant oscillations are  $\omega_{H2}$  and  $\omega_L$  (and its higher harmonics) [Fig. 6(b)]. We therefore predict that both the lower Higgs mode  $\omega_{H2}$  and the Leggett mode  $\omega_L$  can be observed in THz pump-THz probe experiments as oscillations of the pump-probe conductivity, in particular at the gap edge  $2\Delta_2^\infty/\hbar$  and the Leggett mode frequency  $\omega_L$ . The higher Higgs mode  $\omega_{H1}$ , on the other hand, is not visible in the pump-probe signal, since it is strongly damped by the two-particle continuum.

## Discussion

Using a semi-numerical method based on the density matrix approach, we have studied the non-equilibrium ex-

citation of Higgs and Leggett modes in two-band superconductors. While the amplitude Higgs and the Leggett phase mode are decoupled in equilibrium, we find that the out-of-equilibrium excitation process leads to a strong coupling between these two collective modes. As a result, the Leggett phase mode  $\omega_L$  is pushed below the Bogoliubov quasiparticle continuum and remains undamped for a wide range of interband couplings (Figs. 3 and 4). Likewise, the lower Higgs mode  $\omega_{H2}$  is only weakly damped, since its frequency is at the threshold to the quasiparticle continuum. In order to maximize the oscillatory signal of these collective modes in the pump-probe spectra, it is necessary to choose the experimental parameters as follows: (i) the pump-pulse duration  $\tau$  should be smaller than the intrinsic response time of the superconductor  $\hbar/(2|\Delta_i|)$ , such that the collective modes are excited in a non-adiabatic fashion; (ii) the pump-pulse energy needs to be of the order of the superconducting gap (i.e., in the terahertz regime), so that Bogoliubov quasiparticles are excited across the gap, but modes at higher energies  $\hbar\omega \gg |\Delta_i|$  are not populated; and (iii) the pump-pulse intensity must not exceed a few nJ/cm<sup>2</sup> to ensure that the superconducting condensate is only partially broken up, but not completely destroyed. We have predicted that under these conditions both Higgs and Leggett modes can be observed as clear oscillations in the time-resolved pump-probe absorption spectra (Fig. 6). Similarly, we expect that collective mode oscillations are visible in other pump-probe-type experiments, for example in time-resolved photoemission spectroscopy or time-resolved Raman scattering.

It would be intriguing to extend the present study to unconventional exotic superconductors, where several competing orders are present, such as heavy fermion superconductors or high-temperature cuprate and pnictide superconductors. In these systems the pump pulse could be used to induce a transition from one competing order to another. Furthermore, the unconventional pairing symmetries of these superconductors, such as the  $d_{x^2-y^2}$ -wave pairing of the cuprates, give rise to a multitude of new Higgs modes [42]. Our work indicates that non-adiabatic excitation processes will induce interactions among these novel Higgs modes, which await to be further explored both theoretically and experimentally.

## Methods

**Model definition.** The gap equations for the BCS Hamiltonian  $H_{\text{BCS}}$  (see Eq. (1) in the main text) are given by [43]

$$\begin{aligned} \Delta_1 &= \sum_{\mathbf{k}' \in \mathcal{W}} \left( V_1 \langle c_{-\mathbf{k}', \downarrow, 1} c_{\mathbf{k}', \uparrow, 1} \rangle + V_{12} \langle c_{-\mathbf{k}', \downarrow, 2} c_{\mathbf{k}', \uparrow, 2} \rangle \right), \\ \Delta_2 &= \sum_{\mathbf{k}' \in \mathcal{W}} \left( V_2 \langle c_{-\mathbf{k}', \downarrow, 2} c_{\mathbf{k}', \uparrow, 2} \rangle + V_{12} \langle c_{-\mathbf{k}', \downarrow, 1} c_{\mathbf{k}', \uparrow, 1} \rangle \right), \end{aligned} \quad (3)$$

where  $V_1$  and  $V_2$  denote the intraband interactions and  $V_{12} = vV_1$  is the interband coupling. The two-band su-

perconductor is brought out of equilibrium via the coupling to a pump pulse, which is modeled by

$$H_{\text{Laser}} = \frac{e\hbar}{2} \sum_{\mathbf{k}, \mathbf{q}, \sigma, l} \frac{(2\mathbf{k} + \mathbf{q})\mathbf{A}_{\mathbf{q}}(t)}{m_l} c_{\mathbf{k}+\mathbf{q}, \sigma, l}^\dagger c_{\mathbf{k}, \sigma, l} \quad (4)$$

$$+ \frac{e^2}{2} \sum_{\mathbf{k}, \mathbf{q}, \sigma, l} \frac{\left(\sum_{\mathbf{q}'} \mathbf{A}_{\mathbf{q}-\mathbf{q}'}(t)\mathbf{A}_{\mathbf{q}'}(t)\right)}{m_l} c_{\mathbf{k}+\mathbf{q}, \sigma, l}^\dagger c_{\mathbf{k}, \sigma, l},$$

where  $m_l$  is the effective electron mass of the  $l$ th band and  $\mathbf{A}_{\mathbf{q}}(t)$  represents the transverse vector potential of the pump laser. We consider a Gaussian pump pulse described by

$$\mathbf{A}_{\mathbf{q}}(t) = \mathbf{A}_0 e^{-\left(\frac{2\sqrt{\ln 2}t}{\tau}\right)^2} (\delta_{\mathbf{q}, \mathbf{q}_0} e^{-i\omega_0 t} + \delta_{\mathbf{q}, -\mathbf{q}_0} e^{i\omega_0 t}), \quad (5)$$

with central frequency  $\omega_0$ , pulse width  $\tau$ , light-field amplitude  $\mathbf{A}_0 = |\mathbf{A}_0|\hat{\mathbf{e}}_y$ , and photon wave-vector  $\mathbf{q}_0 = q_0\hat{\mathbf{e}}_x$ .

**Density matrix formalism.** In order to simulate the nonequilibrium dynamics of the two-band superconductor (1), we use a semi-numerical method based on the density matrix formalism. This approach involves the analytical derivation of equations of motions for the Bogoliubov quasiparticle densities  $\langle \alpha_{\mathbf{k}, l}^\dagger \alpha_{\mathbf{k}', l} \rangle$ ,  $\langle \beta_{\mathbf{k}, l}^\dagger \beta_{\mathbf{k}', l} \rangle$ ,  $\langle \alpha_{\mathbf{k}, l}^\dagger \beta_{\mathbf{k}', l}^\dagger \rangle$ , and  $\langle \alpha_{\mathbf{k}, l} \beta_{\mathbf{k}', l} \rangle$ , which are then integrated up numerically using a Runge Kutta algorithm. The Bogoliubov quasiparticle densities are defined in terms of the fermionic operators  $\alpha_{\mathbf{k}, l}$  and  $\beta_{\mathbf{k}, l}$ , with

$$\alpha_{\mathbf{k}, l} = u_{\mathbf{k}, l} c_{\mathbf{k}, l, \uparrow} - v_{\mathbf{k}, l} c_{-\mathbf{k}, l, \downarrow}^\dagger, \quad (6)$$

$$\beta_{\mathbf{k}, l} = v_{\mathbf{k}, l} c_{\mathbf{k}, l, \uparrow}^\dagger + u_{\mathbf{k}, l} c_{-\mathbf{k}, l, \downarrow}, \quad (7)$$

where  $v_{\mathbf{k}, l} = \Delta_l(t_i)/|\Delta_l(t_i)|\sqrt{(1 - \epsilon_{\mathbf{k}, l}/E_{\mathbf{k}, l})/2}$ ,  $u_{\mathbf{k}, l} = \sqrt{(1 + \epsilon_{\mathbf{k}, l}/E_{\mathbf{k}, l})/2}$ , and  $E_{\mathbf{k}, l} = \sqrt{\epsilon_{\mathbf{k}, l}^2 + |\Delta_l(t_i)|^2}$ . We emphasize that the coefficients  $u_{\mathbf{k}, l}$  and  $v_{\mathbf{k}, l}$  do not depend on time, i.e., the temporal evolution of the quasiparticle densities is computed with respect to a fixed time-independent Bogoliubov-de Gennes basis in which the initial state is diagonal. The equations of motion for the quasiparticle densities are readily obtained from Heisenberg's equation of motion. Since Eq. (1) represents a mean-field Hamiltonian, this yields a closed system of

differential equations, and hence no truncation is needed (for details see, e.g., Refs. [16, 22, 24, 27]).

**Pump-probe response.** All physical observables, such as the current density  $\mathbf{j}_{\mathbf{q}_{\text{pr}}}(\delta t, t)$ , can be expressed in terms of the quasiparticle densities. For the current density we find that

$$\mathbf{j}_{\mathbf{q}_{\text{pr}}}(\delta t, t) = \frac{-e\hbar}{2mV} \sum_{\mathbf{k}, l, \sigma} (2\mathbf{k} + \mathbf{q}_{\text{pr}}) \langle c_{\mathbf{k}, l, \sigma}^\dagger c_{\mathbf{k}+\mathbf{q}_{\text{pr}}, l, \sigma} \rangle(\delta t, t)$$

$$- \frac{e^2}{mV} \sum_{\mathbf{k}, l, \mathbf{q}, \sigma} \mathbf{A}_{\mathbf{q}_{\text{pr}}-\mathbf{q}} \langle c_{\mathbf{k}, l, \sigma}^\dagger c_{\mathbf{k}+\mathbf{q}, l, \sigma} \rangle(\delta t, t), \quad (8)$$

where  $\mathbf{A}_{\mathbf{q}_{\text{pr}}}(\delta t, t)$  and  $\mathbf{q}_{\text{pr}} = |\mathbf{q}_{\text{pr}}|\hat{\mathbf{e}}_x$  are the vector potential and the wave vector of the probe pulse, respectively. With this, we obtain the pump-probe conductivity via [22, 44]

$$\sigma(\delta t, \omega) = \frac{j(\delta t, \omega)}{i\omega A(\delta t, \omega)}, \quad (9)$$

where  $j(\delta t, \omega)$  and  $A(\delta t, \omega)$  denote the Fourier transformed  $y$  components of the current density  $\mathbf{j}_{\mathbf{q}_{\text{pr}}}(\delta t, t)$  and the vector potential  $\mathbf{A}_{\mathbf{q}_{\text{pr}}}(\delta t, t)$ , respectively. To compute the effects of the probe pulse, we neglect terms of second order and higher in the probe field  $A_{\text{pr}}(t)$ , since the probe pulse has a very weak intensity.

**Numerical discretization and integration.** To keep the number of equations of motion manageable, we have to restrict the number of considered points in momentum space. The first restriction is that we only take expectation values with indices  $\mathbf{k}$  and  $\mathbf{k} + \mathbf{q} \in \mathcal{W}$  into account. This means that we concentrate on the  $\mathbf{k}$ -values where the attractive pairing interaction takes place. Furthermore, since the external electromagnetic field may add or subtract only momentum  $n\mathbf{q}_0$ , it is sufficient to consider expectation values with indices  $(\mathbf{k}, \mathbf{k} + n\mathbf{q}_0)$ , where  $n \in \mathbb{Z}$ . For small amplitudes  $|\mathbf{A}_{\mathbf{q}_0}|$  the off-diagonal elements of the quasiparticle densities decrease rapidly as  $n$  increases, since  $(\mathbf{k}, \mathbf{k} + n\mathbf{q}_0) = O(|\mathbf{A}_{\mathbf{q}_0}|^{|n|})$ . Thus, we set all entries with  $n > 4$  to zero. With this momentum-space discretization, we obtain of the order of  $10^5$  equations, which we are able to solve numerically using high-efficiency parallelization. Further, technical details can be found in Refs. [22, 24].

- 
- [1] Matsunaga, R. & Shimano, R. Nonequilibrium bcs state dynamics induced by intense terahertz pulses in a superconducting nbn film. *Phys. Rev. Lett.* **109**, 187002 (2012).
- [2] Matsunaga, R. et al. Higgs amplitude mode in the bcs superconductors nb<sub>1-x</sub>ti<sub>x</sub>N induced by terahertz pulse excitation. *Phys. Rev. Lett.* **111**, 057002 (2013).
- [3] Matsunaga, R. et al. Light-induced collective pseudospin precession resonating with higgs mode in a superconduc-

- tor. *Science* **345**, 1145–1149 (2014).
- [4] Mansart, B. et al. Coupling of a high-energy excitation to superconducting quasiparticles in a cuprate from coherent charge fluctuation spectroscopy. *Proc. Natl. Acad. Sci. USA* **110**, 4539–4544 (2013).
- [5] Pashkin, A. & Leitenstorfer, A. Particle physics in a superconductor. *Science* **345**, 1121–1122 (2014).
- [6] Dal Conte, S. et al. Disentangling the electronic and phononic glue in a high-*t<sub>c</sub>* superconductor. *Science* **335**,

- 1600–1603 (2012).
- [7] Beck, M. *et al.* Transient increase of the energy gap of superconducting nbn thin films excited by resonant narrow-band terahertz pulses. *Phys. Rev. Lett.* **110**, 267003 (2013).
- [8] Pashkin, A. *et al.* Femtosecond response of quasiparticles and phonons in superconducting  $\text{YBa}_2\text{Cu}_3\text{O}_{7-x}$  studied by wideband terahertz spectroscopy. *Phys. Rev. Lett.* **105**, 067001 (2010).
- [9] Beck, M. *et al.* Energy-gap dynamics of superconducting nbn thin films studied by time-resolved terahertz spectroscopy. *Phys. Rev. Lett.* **107**, 177007 (2011).
- [10] Hellmann, S. *et al.* Time-domain classification of charge-density-wave insulators. *Nat Commun* **3**, 1069 (2012).
- [11] Torchinsky, D. H., Mahmood, F., Bollinger, A. T., Božović, I. & Gedik, N. Fluctuating charge-density waves in a cuprate superconductor. *Nat Mater* **12**, 387–391 (2013).
- [12] Kimel, A. V., Kirilyuk, A., Tsvetkov, A., Pisarev, R. V. & Rasing, T. Laser-induced ultrafast spin reorientation in the antiferromagnet  $\text{tmfco}_3$ . *Nature* **429**, 850–853 (2004).
- [13] Amin, M. H. S., Bezuglyi, E. V., Kijko, A. S. & Omelyanchouk, A. N. Wigner distribution function formalism for superconductors and collisionless dynamics of the superconducting order parameter. *Low Temperature Physics* **30**, 661–666 (2004).
- [14] Volkov, A. F. & Kogan, S. M. Collisionless relaxation of the energy gap in superconductors. *Sov. Phys. JETP* **38**, 1018 (1974).
- [15] Schnyder, A. P., Manske, D. & Avella, A. Resonant generation of coherent phonons in a superconductor by ultrafast optical pump pulses. *Phys. Rev. B* **84**, 214513 (2011).
- [16] Papenkort, T., Axt, V. M. & Kuhn, T. Coherent dynamics and pump-probe spectra of bcs superconductors. *Phys. Rev. B* **76**, 224522 (2007).
- [17] Papenkort, T., Kuhn, T. & Axt, V. M. Coherent control of the gap dynamics of bcs superconductors in the nonadiabatic regime. *Phys. Rev. B* **78**, 132505 (2008).
- [18] Yuzbashyan, E. A., Tsyplatyev, O. & Altshuler, B. L. Relaxation and persistent oscillations of the order parameter in fermionic condensates. *Phys. Rev. Lett.* **96**, 097005 (2006).
- [19] Yuzbashyan, E. A., Altshuler, B. L., Kuznetsov, V. B. & Enolskii, V. Z. Nonequilibrium cooper pairing in the nonadiabatic regime. *Phys. Rev. B* **72**, 220503 (2005).
- [20] Yuzbashyan, E. A., Altshuler, B. L., Kuznetsov, V. B. & Enolskii, V. Z. Solution for the dynamics of the bcs and central spin problems. *Journal of Physics A: Mathematical and General* **38**, 7831 (2005).
- [21] Zachmann, M. *et al.* Ultrafast terahertz-field-induced dynamics of superconducting bulk and quasi-1d samples. *New Journal of Physics* **15**, 055016 (2013).
- [22] Krull, H., Manske, D., Uhrig, G. S. & Schnyder, A. P. Signatures of nonadiabatic BCS state dynamics in pump-probe conductivity. *Phys. Rev. B* **90**, 014515 (2014).
- [23] Yuzbashyan, E. A., Dzero, M., Gurarie, V. & Foster, M. S. Quantum quench phase diagrams of an  $s$ -wave bcs-bec condensate. *Phys. Rev. A* **91**, 033628 (2015).
- [24] Krull, H. *Conductivity of strongly pumped superconductors*. Ph.D. thesis, TU Dortmund (2014). URL <http://hdl.handle.net/2003/33996>.
- [25] Kemper, A. F., Sentef, M. A., Moritz, B., Freericks, J. K. & Devereaux, T. P. Amplitude mode oscillations in pump-probe photoemission spectra of electron-phonon mediated superconductors. *ArXiv e-prints* (2014). 1412.2762.
- [26] Peronaci, F., Schirò, M. & Capone, M. Transient Dynamics of  $d$ -wave Superconductors after a Sudden Excitation. *ArXiv e-prints* (2015). 1506.01409.
- [27] Akbari, A., Schnyder, A. P., Manske, D. & Eremin, I. Theory of nonequilibrium dynamics of multiband superconductors. *Europhys. Lett.* **101**, 17002 (2013).
- [28] Dzero, M., Khodas, M. & Levchenko, A. Amplitude modes and dynamic coexistence of competing orders in multicomponent superconductors. *Phys. Rev. B* **91**, 214505 (2015).
- [29] Demsar, J. *et al.* Pair-breaking and superconducting state recovery dynamics in  $\text{MgB}_2$ . *Phys. Rev. Lett.* **91**, 267002 (2003).
- [30] Leggett, A. J. Number-phase fluctuations in two-band superconductors. *Progress of Theoretical Physics* **36**, 901–930 (1966).
- [31] Burnell, F. J., Hu, J., Parish, M. M. & Bernevig, B. A. Leggett mode in a strong-coupling model of iron arsenide superconductors. *Phys. Rev. B* **82**, 144506 (2010).
- [32] Anishchanka, A., Volkov, A. F. & Efetov, K. B. Collective modes in two-band superconductors in the dirty limit. *Phys. Rev. B* **76**, 104504 (2007).
- [33] Pekker, D. & Varma, C. Amplitude/higgs modes in condensed matter physics. *Annual Review of Condensed Matter Physics* **6**, 269–297 (2015).
- [34] Anderson, P. W. Random-phase approximation in the theory of superconductivity. *Phys. Rev.* **112**, 1900–1916 (1958).
- [35] Bogoliubov, N. N., Tolmatshev, V. V. & Shirkov, D. V. *New Method in the Theory of Superconductivity* (Consultants Bureau, New York, 1959).
- [36] Podolsky, D., Auerbach, A. & Arovas, D. P. Visibility of the amplitude (higgs) mode in condensed matter. *Phys. Rev. B* **84**, 174522 (2011).
- [37] Sooryakumar, R. & Klein, M. V. Raman scattering by superconducting-gap excitations and their coupling to charge-density waves. *Phys. Rev. Lett.* **45**, 660–662 (1980).
- [38] Littlewood, P. B. & Varma, C. M. Gauge-invariant theory of the dynamical interaction of charge density waves and superconductivity. *Phys. Rev. Lett.* **47**, 811–814 (1981).
- [39] Blumberg, G. *et al.* Observation of leggett’s collective mode in a multiband  $\text{mgb}_2$  superconductor. *Phys. Rev. Lett.* **99**, 227002 (2007).
- [40] Méasson, M.-A. *et al.* Amplitude higgs mode in the  $2h$ – $\text{nbse}_2$  superconductor. *Phys. Rev. B* **89**, 060503 (2014).
- [41] Sharapov, S. G., Gusynin, V. P. & Beck, H. Effective action approach to the leggett’s mode in two-band superconductors. *Eur. Phys. J. B* **30**, 45–51 (2002).
- [42] Barlas, Y. & Varma, C. M. Amplitude or higgs modes in  $d$ -wave superconductors. *Phys. Rev. B* **87**, 054503 (2013).
- [43] Suhl, H., Matthias, B. T. & Walker, L. R. Bardeen-cooper-schrieffer theory of superconductivity in the case of overlapping bands. *Phys. Rev. Lett.* **3**, 552–554 (1959).
- [44] Shao, C., Tohyama, T., Luo, H.-G. & Lu, H. A nu-

merical method to compute optical conductivity based on the pump-probe simulations. [ArXiv e-prints](#) (2015). 1507.01200.

### **Acknowledgements**

We gratefully acknowledge many useful discussions with A. Avella, S. Kaiser and R. Shimano. G.S.U. and H.K. acknowledge financial support by the DFG in TRR 160. H.K. thanks the Max-Planck-Institut FKF Stuttgart for its hospitality.

### **Competing financial interests**

The authors declare that they have no competing financial interests.

### **Author contributions**

The density matrix simulations were developed and run by H.K., N.B., and A.P.S. All authors contributed to the discussion and interpretation of the results and to the writing of the paper.